Supporting Information

Ditungsten Carbide Nanoparticles Encapsulated by Ultrathin Graphitic Layers with Excellent Hydrogen-Evolution Electrocatalytic Properties

Yao Zhou,[1] Ruguang Ma,[1] Pengxi Li,[1] Yongfang Chen,[1] Qian Liu,[,1] Guozhong Cao,[*,2,3] and Jiacheng Wang[*,1]*

1 The State Key Laboratory of High Performance Ceramics and Superfine Microstructure, Shanghai Institute of Ceramics, Chinese Academy of Sciences, 1295 Dingxi Road, Shanghai, 200050, P. R. China

2 Department of Materials Science and Engineering, University of Washington, Seattle, WA 98195, USA

3 Beijing Institute of Nanoenergy and Nanosystems, Chinese Academy of Sciences, Beijing, 100083, P. R. China

* Author for correspondence. Email: gzcao@u.washington.edu; qianliu@sunm.shcnc.ac.cn; jiacheng.wang@mail.sic.ac.cn, Tel: 86-21-52412714, Fax: 86-21-52413122

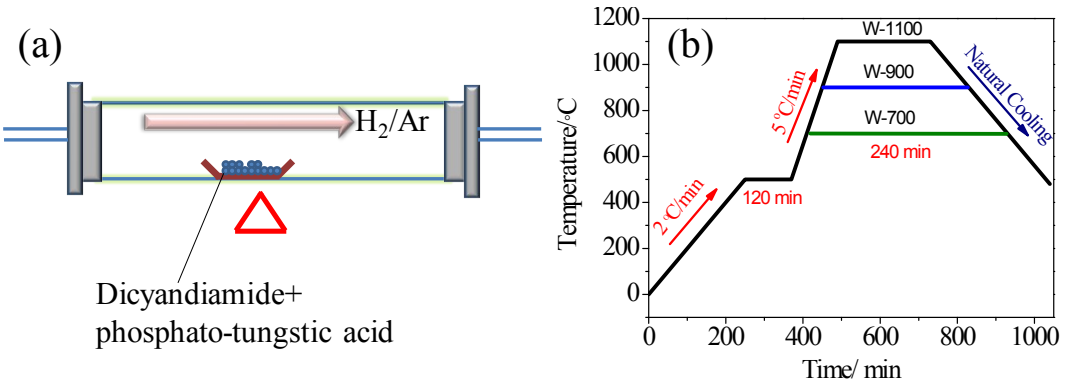

Figure S1. (a) Schematic diagram of the apparatus used for the synthesis of W-700, W-900 and W-1100; (b) temperature program applied for the synthesis of nanoelectrocatalyst.

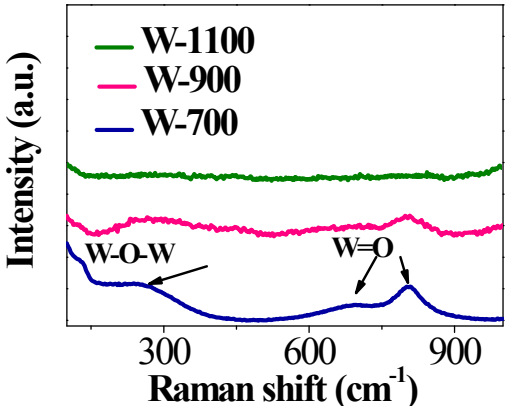

Figure S2. Raman spectra of samples W-700, W-900 and W-1100 at low Raman shift area.

The spectrum of W-700 and W-900 samples displays characteristic Raman peaks at 260, 707 and 808 cm^{-1}, that can be assigned to W-O-W deformation mode, the W=O bending mode and the W=O stretching mode in WO_3, repectively.[1] With pyrolysis treatment at 900 °C for 4 h, the peaks assigned to WO_3 get weaker. At 1100 °C, the WO_3 peaks are completely vanished, which verifies the successful chemical conversion from

WO_3 to W_2C via pyrolysis process.

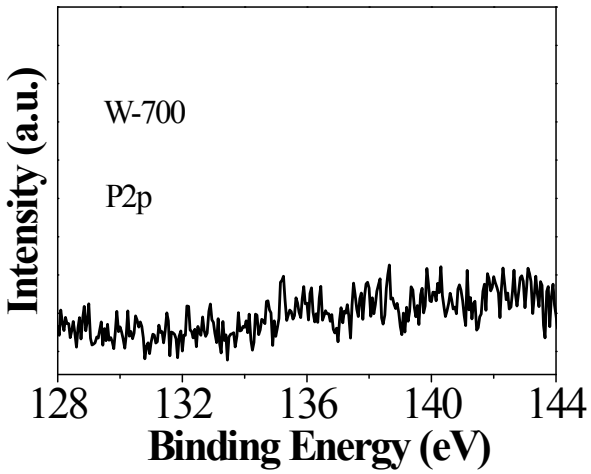

Figure S3. The high resolution XPS spectra of P 2p for sample W-700.

Phosphorus, which should have been introduced from precursor (phosphotungstic acid) is not detected in W-700 with pyrolysis temperature at 700 °C. It is believed that phosphorus is unstable and ready to be evaporated with heat-treatment.[2] The complete phosphorus removal of the W-700 suggests no existence of P in the samples with pyrolysis temperatures above 700 °C.

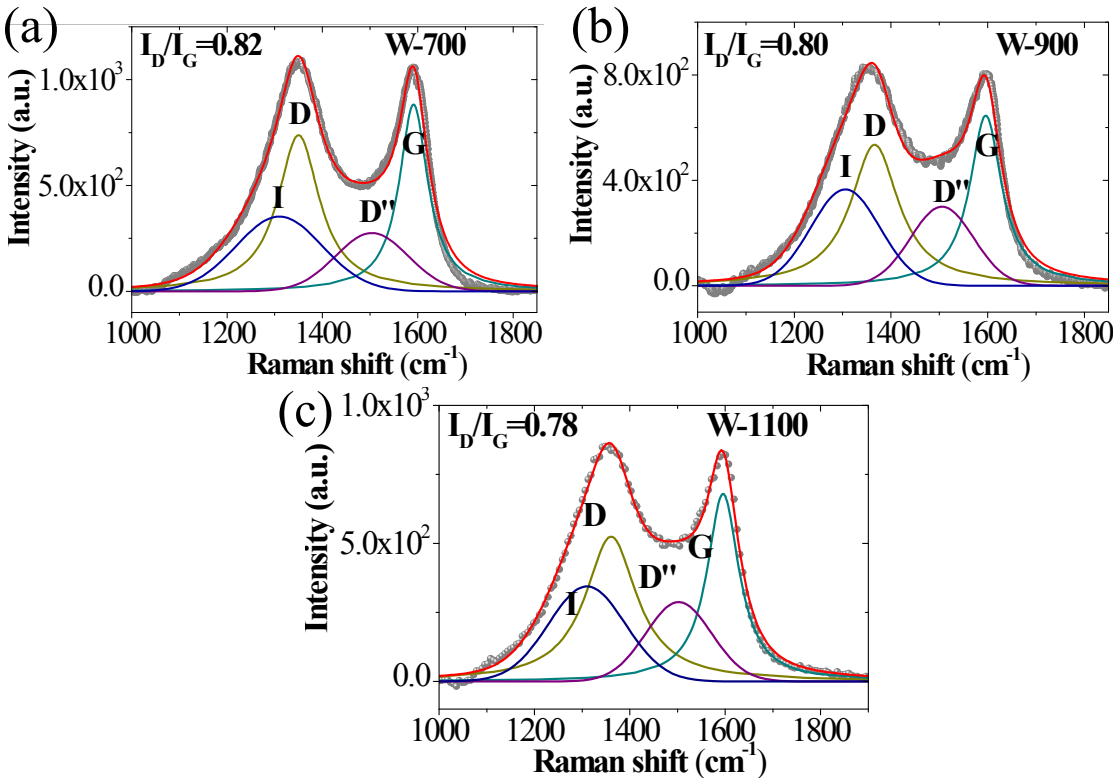

Figure S4. Deconvoluted Raman spectra of (a) W-700, (b) W-900, and (c) W-1100 showing D, G, I and D'' bands with values of I_D/I_G.

All samples had the similar main features of graphitic materials. The G band stems from in-plane vibrations and has E_{2g} symmetry. This is observed in all sp^2 carbon systems. The D band stems from a double resonance process involving a phonon and a defect. After fitting process, additional bands are labeled as I and D''. The I band is linked with disorder in the graphitic lattice, sp^2-sp^3 bonds or the presence of polyenes at ~1180-1290 cm^{-1}.[3] The D'' band (~1500 cm^{-1}) is known to occur in the presence of amorphous carbon.[4]

Table S1. Elemental composition of samples W-x.

Sample	C (at%)	W (at%)	O (at%)
W-700	56.5	10.0	33.5
W-900	68.9	11.2	18.9
W-1100	72.2	21.7	6.1

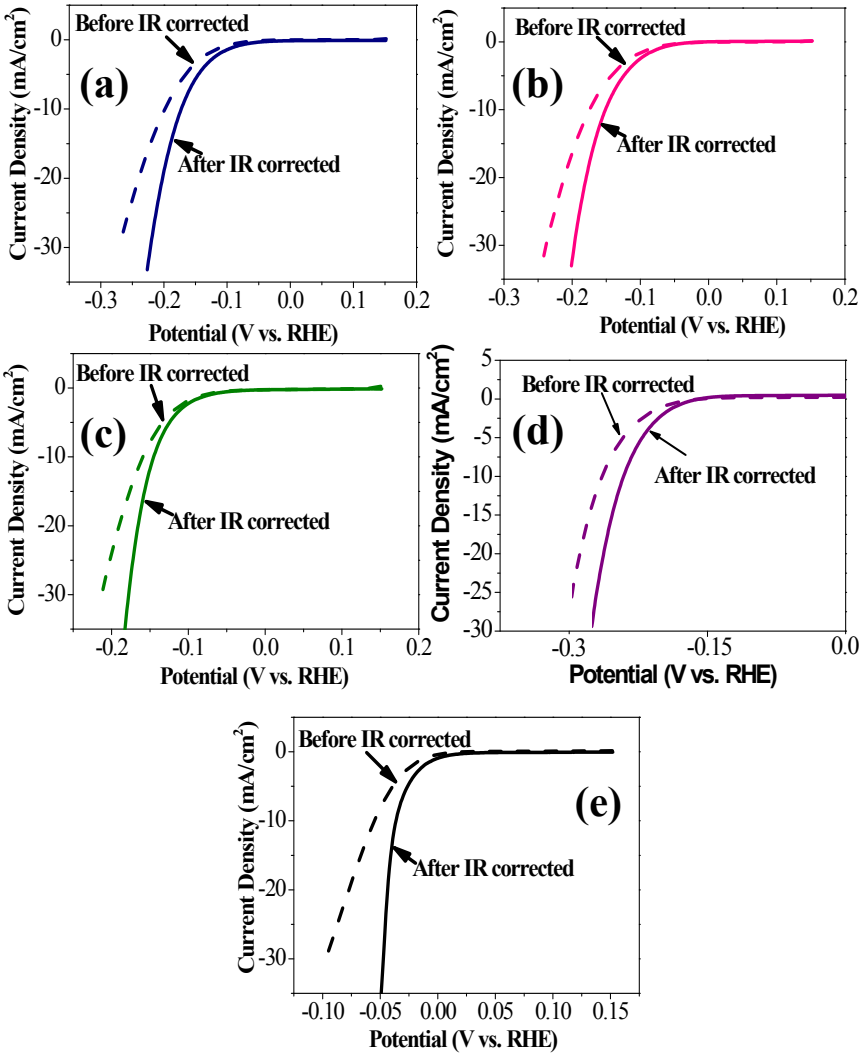

Figure S5. Polarization curves of (a) W-700, (b) W-900, (c) W-1100 (d) pristine graphene and (e) 20% Pt/C before and after 90% *iR* compensation.

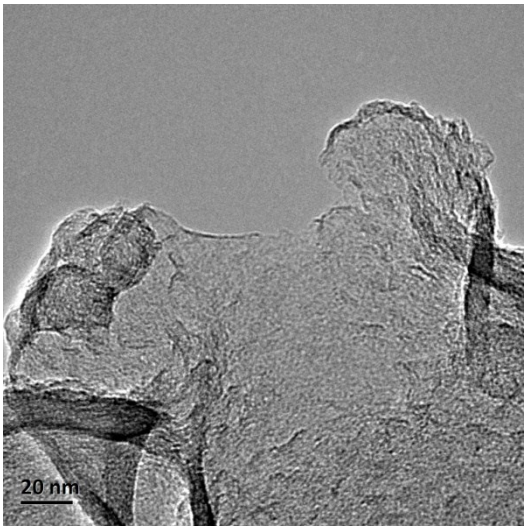

Figure S6. TEM image of as-prepared pristine graphene.

Table S2. Nitrogen sorption data from pristine graphene.

Sample ID	S_{BET} (m^2/g)	S_{Meso}	S_{Micro}	V_{Meso} (cm^3/g)	V_{Micro}
Prstine graphene	170.0	118.1	73.9	0.39	0.33

It shows that the specific surface area of pristine graphene (170.0 m^2/g) is larger than those of W-x samples. It is believed that the higher surface area of catalyst facilitate to increased effective active surface, leading to enhanced catalytic performance. Without the promoting effect of W_2C phase, only considering the contribution of surface area, pristine graphene should have exhibited the best catalytic performance. However, W-x samples all perform better than pristine graphene, indicating the apparent enhanced catalytic activity induced by W-containing nanoparticles.

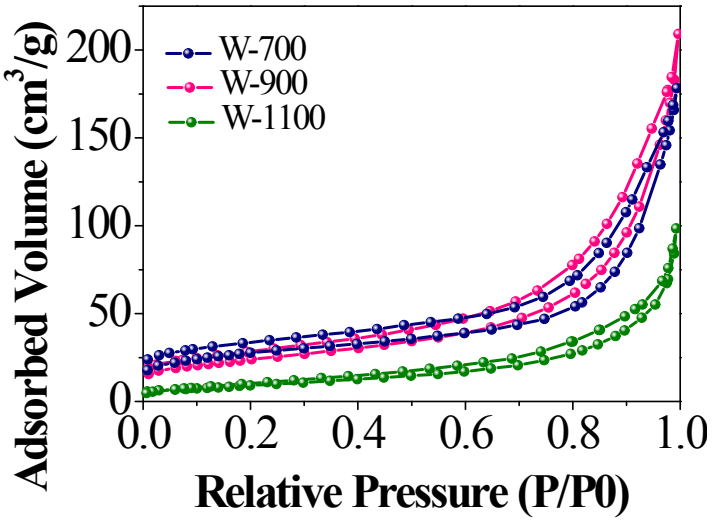

Figure S7. N_2 adsorption-desorption isotherms of samples W-x.

Table S3. Nitrogen sorption data from samples W-700, W-900 and W-1100.

Sample ID	S_{BET} (m^2/g)	S_{Meso}	S_{Micro}	V_{Meso} (cm^3/g)	V_{Micro}
W-700	136.5	101.4	34.6	0.26	0.01
W-900	117.4	97.2	8.9	0.32	0.01
W-1100	45.7	39.7	3.2	0.16	0.01

Nitrogen sorption was used to determine the surface area and pore volume of WO_3/W_2C@GL samples. The samples exhibit type IV isotherms with shape H4 type hysteresis loop. It is believed that the H4 is associated with the existence of narrow slit-like pores.[29] In addition, with increased pyrolysis temperature, micropores tends to be melted due to the vanishing of diverge of isotherms at relative pressures (P/P0) below 0.2.

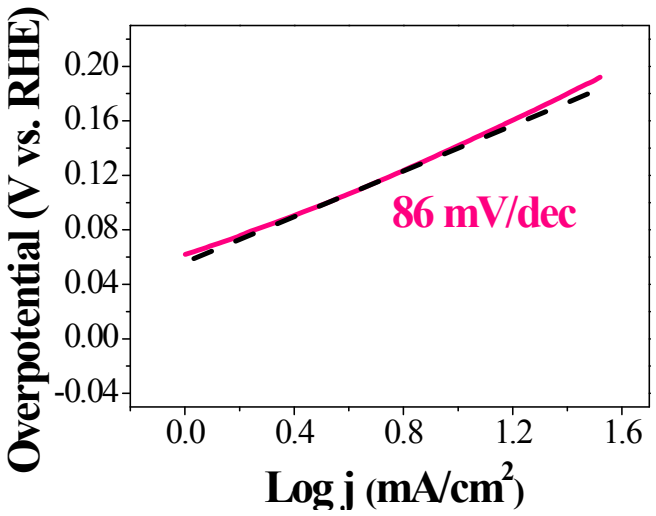

Figure S8. Tafel plot of W-900 in 0.5 M H_2SO_4 acidic solution.

Table S4. Comparison of the electrocatalytic activity of the W-1100 reported here under acidic conditions with other non-noble transition metal HER electrocatalysts.

Sample ID	j_0 (mA cm^{-2})	η_{10} (mV)	Oneset potential (mV)	Loading of catalyst (mg cm^{-2})	Tafel slope (mV dec^{-1})	Ref.
W-1100	**0.24**	**135**	**40**	**0.5**	**68**	**This work**
W_2C microspheres	2.8×10^{-4}	190	85	--	118	5
W_2C nanoparticles	--	200	--	263	--	6
WC/aligned carbon tubes	--	145	15	0.2	72	7
β-Mo_2C	0.0173	--	50	0.28	120	8
γ-Mo_2C	0.0032	--	80	0.28	121.6	8
Commercial Mo_2C	0.0013	192	--	339	56	9
β-Mo_2C/reduced graphene oxide	0.037	109	20	0.47	66.4	10
WC nanocrystals	0.28	125	--	1	84	11
Mo_2C/CNT-graphene	0.062	130	62	0.66	58	12
WS_2 nanosheets	--	142	100	1	70	13
Chemically exfoliated WS_2 nanosheets	0.02	230	80	0.0015	55	14
Metallic MoS_2 nanosheets	--	187	150	--	43	15
Co@NCNTs	0.01	270	50	0.28	69	16
FeCo@NCNTs	--	280	110	0.32	72	17
Ni_2P nanoparticles	0.49	100	20	0.033	46	18
Co_2P nanorods	0.025	134	70	1.02	51.7	19

MoP	0.086	150	40	0.39	54	20
P-WN/rGO	0.35	85	46	0.337	54	21
Metallic WO_2/carbon	0.64	58	35	0.35	46	22
MoCN NPs	--	140	50	0.4	46	23
Commercial MoB	0.0014	220	>100	339	55	24
MoP	0.034	130	50	0.86	54	25
Amorphous MoP nanoparticles	0.12	90	--	1	45	26
CoP nanoparticles	0.14	75	20	2	50	27
Ni-Mo nitrides	0.24	--	78	0.25	35.9	28

Table S5. HER catalytic properties of W-x samples.

Sample ID	η_{10} (mV)	Oneset potential (mV)	Tafel slope (mV dec^{-1})
W-700	175	80	92
W-900	151	55	86
W-1100	135	40	68

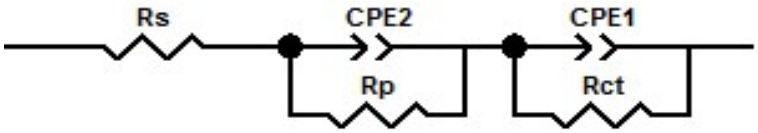

Figure S9. Electrical equivalent circuit model for fitting the EIS response of hydrogen evolution reaction on W-x samples with different pyrolysis temperatures and amount of phosphotungstic acid. The whole model follows the two-time constant model, where R_s, is the series resistance, R_{ct} denotes the charge transfer resistance, R_p related to is the porosity the electrode surface.

The model consists of a series resistance, Rs, in series with two parallel branches; one is related to the charge-transfer process (CPE_1-R_{ct}); the other is on the surface porosity. W-1100 exhibits a much lower charge transfer resistance (16.9 Ω) than W-700 (42.3 Ω) and W-900 (32.4 Ω).

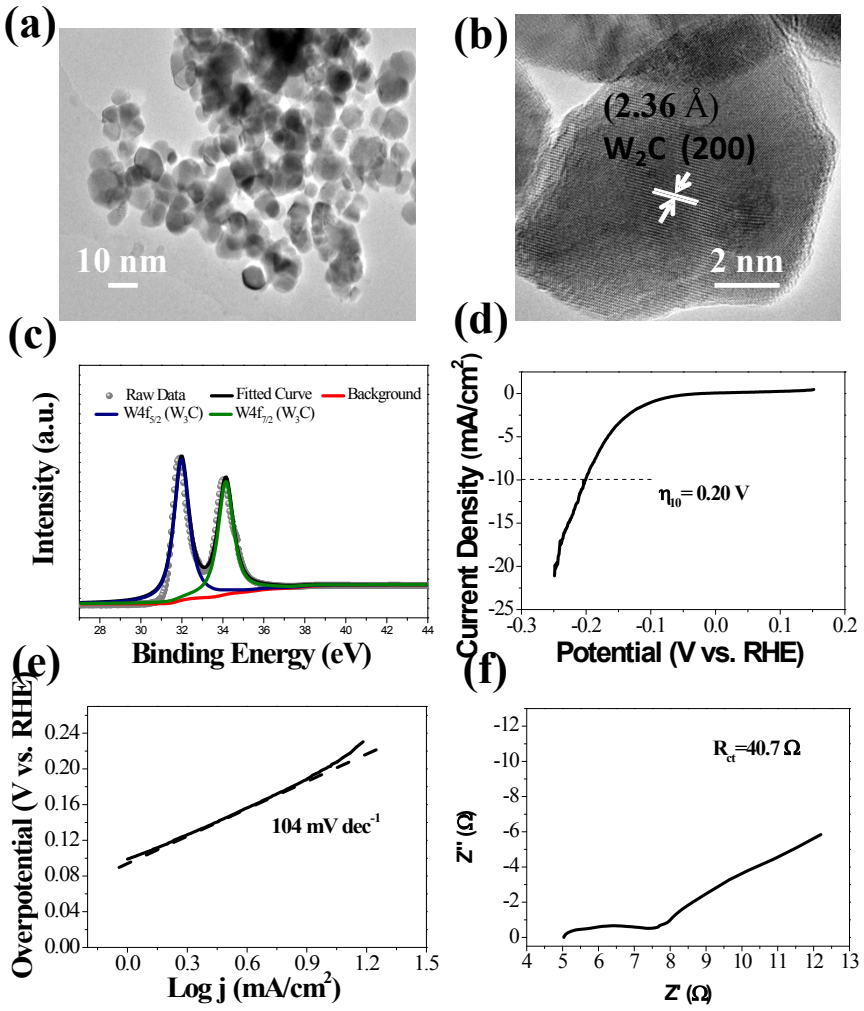

Figure S10. (a), (b) TEM images of W_2C NP without GL wrapping; (c) high resolution XPS spectrum of W 4f for the f-W_2C-1100; (d) LSV polarization curve and (e) corresponding Tafel plot of W_2C NP without GL wrapping pyrolyzed at 1100 °C in 0.5 M H_2SO_4 at scan rates of 2 mV s^{-1}.

Reference

[1] S. S. Chan, I. E. Wachs, L. L. Murrell, *J. Catal.*, 1984, **90**, 150-155.

[2] G. Larkins, Y. Vlasov, Supercond. *Sci. Tech.*, 2011, **24**, 092001.

[3] W. S. Bacsa, J. S. Lannin, D. L. Pappas, J. J. Cuomo, *Rev. B*, 1993, **47**, 10931.

[4] T. Jawhari, A. Roig, J. Casado, *Carbon*, 1995, **33**, 1561-1565.

[5] D. J. Ham, R. Ganesan, J. S. Lee, *Int. J. Hydrogen Energy*, 2008, **33**, 6865-6872.

[6] F. Harnisch, G. Sievers, U. Schroder, *Appl. Catal. B-Environ.*, 2009, **89**, 455-458.

[7] X. J. Fan, H. Q. Zhou, X. Guo, *ACS Nano*, 2015, **9**, 5125-5134.

[8] C. Wan, Y. N. Regmi, B. M. Leonard, Angew. Chem. Int. Edit. 53 (2014) 6407-6410.

[9] H. Vrubel, X. L. Hu, *Angew. Chem. Int. Edit.*, 2012, **51**, 12703-12706.

[10] W. F. Chen, S. Iyer, K. Sasaki, C. H. Wang, Y. M. Zhu, J. T. Muckerman, E. Fujita, *Energy Environ. Sci.*, 2013, **6**, 1818-1826.

[11] A. T. Garcia-Esparza, D. Cha, Y. W. Ou, J. Kubota, K. Domen, K. Takanabe, *Chemsuschem*, 2013, **6**, 168-181.

[12] D. H. Youn, S. Han, J. Y. Kim, H. Park, S. H. Choi, J. S. Lee, *ACS Nano*, 2014, **8**, 5164-5173.

[13] M. A. Lukowski, A. S. Daniel, C. R. English, F. Meng, A. Forticaux, R. J. Hamers, S. Jin, *Energy Environ. Sci.*, 2014, **7**, 2608-2613.

[14] D. Voiry, H. Yamaguchi, J. Li, R. Silva, D. C. B. Alves, T. Fujita, M. Chen, T. Asefa, V. B. Shenoy, G. Eda, M. Chhowalla, *Nat. Mater.*, 2013, **12**, 850-855.

[15] M. A. Lukowski, A. S. Daniel, F. Meng, A. Forticaux, L. S. Li, S. Jin, *J. Am. Chem. Soc.*, 2013, **135**, 10274-10277.

[16] X. X. Zou, X. X. Huang, A. Goswami, R. Silva, B. R. Sathe, E. Mikmekova, T. Asefa, *Angew. Chem. Int. Edit.*, 2014, **53**, 4372-4376.

[17] J. Deng, P. J. Ren, D. H. Deng, L. Yu, F. Yang, X. H. Bao, *Energy Environ. Sci.*, 2014, **7**, 1919-1923.

[18] E. J. Popczun, J. R. McKone, C. G. Read, A. J. Biacchi, A. M. Wiltrout, N. S. Lewis, R. E. Schaak, *J. Am. Chem. Soc.*, 2013, **135**, 9267-9270.

[19] Z. P. Huang, Z. Z. Chen, Z. B. Chen, C. C. Lv, M. G. Humphrey, C. Zhang, *Nano Energy*, 2014, **9**, 373-382.

[20] Z. C. Xing, Q. Liu, A. M. Asiri, X. P. Sun, *Adv. Mater.*, 2014, **26**, 5702-5707.

[21] H. J. Yan, C. G. Tian, L. Wang, A. P. Wu, M. C. Meng, L. Zhao, H. G. Fu, *Angew. Chem. Int. Edit.*, 2015, **54**, 6325-6329.

[22] R. Wu, J. F. Zhang, Y. M. Shi, D. Liu, B. Zhang, *J. Am. Chem. Soc.*, 2015, **137**, 6983-6986.

[23] Y. Zhao, K. Kamiya, K. Hashimoto, S. Nakanishi, *J. Am. Chem. Soc.*, 2015, **137**, 110-113.

[24] H. Vrubel, X. Hu, *Angew. Chem. Int. Edit.*, 2012, **51**, 12703-12706.

[25] P. Xiao, M. A. Sk, L. Thia, X. Ge, R. J. Lim, J. Y. Wang, K. H. Lim, X. Wang, *Energy Environ. Sci.*, 2014, **7**, 2624-2629.

[26] J. M. McEnaney, J. C. Crompton, J. F. Callejas, E. J. Popczun, A. J. Biacchi, N. S. Lewis, R. E. Schaak, *Chem. Mater.*, 2014, **26**, 4826-4831.

[27] E. J. Popczun, C. J. Read, C. W. Roske, N. S. Lewis, R. E. Schaak, *Angew. Chem.*, 2014, **126**, 5531-5534.

[28] W. F. Chen, K. Sasaki, C. Ma, A. I. Frenkel, N. Narinkovic, J. T. Muckerman, Y. Zhu, R. R. Adzic, *Angew. Chem. Int. Edit.*, 2012, **51**, 6131-6135.

[29] J. W. McBain, *J. Am. Chem. Soc.*, 1935, **57**, 699-700.